BUTTERWORTH HEINEMANN

Polymer Vol. 36 No. 3, pp. 611–620, 1995
Copyright © 1995 Elsevier Science Ltd
Printed in Great Britain. All rights reserved
0032-3861/95/$10.00 + 0.00

Changes of thermodynamic and dynamic mechanical properties of poly(methyl methacrylate) due to structural relaxation: low-temperature ageing and modelling

E. Muzeau*, G. Vigier†, R. Vassoille and J. Perez
Groupe d'Etudes de Métallurgie Physique et de Physique des Matériaux, Institut National des Sciences Appliquées, 69621 Villeurbanne Cedex, France
(Received 6 September 1993)

Structural relaxation of poly(methyl methacrylate) has been studied by differential scanning calorimetric (d.s.c.) and dynamic mechanical techniques, and the effect of temperature of ageing has been investigated. Isothermal ageings at temperatures between $T_g - 30$ K and $T_g - 100$ K lead to d.s.c. pre-peaks and a diminution of the mechanical loss tangent. The β relaxation is not affected by ageing and the α relaxation exhibits a low-temperature tail within the temperature domain of the β relaxation. A physical model based upon the concept of annihilation of quasi-point defects through diffusion is used to analyse the results. Diffusion is thought to occur by means of hierarchically correlated movements characterized by a correlation factor b. Simulation of the calorimetric data is satisfactory and comparison with the dynamic mechanical results underlines a specific mechanism for ageing temperatures far below T_g

(Keywords: poly(methyl methacrylate); structural relaxation; dynamic mechanical properties)

INTRODUCTION

The intrinsic nature of glasses is to be frozen in at a temperature T_g below which they are in a non-equilibrium state. Such systems, when maintained below T_g, spontaneously evolve towards equilibrium in a mechanism called structural relaxation or physical ageing. Structural relaxation affects a variety of properties such as density, enthalpy, volume, complex dielectric permittivity and complex mechanical modulus. This phenomenon has been shown to be closely related to the glass transition kinetics[1].

A variety of empirical equations have been shown to agree with the results of d.s.c. experiments of physical ageing, the first work being that of Tool[2]. Narayanaswamy[3] and Kovacs *et al.*[1] generalized Tool's model by allowing for a distribution of relaxation times. These theories account for the well established non-linearity and the non-exponentiality of the glass transition kinetics, but the relaxation time is described by four parameters that have no physical meaning. Hodge[4] incorporated the Adam–Gibbs equation[5] into Narayanaswamy's model and then attributed a physical meaning to the previous parameters. However, a distribution of elementary relaxation times cannot explain the value of the pre-exponential factor, which is too low to correspond to any physically possible motion.

A number of remarks are to be made regarding these models:

(i) They are phenomenological tools for a good description of the experimental results of physical ageing, but the parameters need to be changed when the thermal history is changed.

(ii) The choice of a relaxation-time distribution (or of β, the exponent of the Kohlrausch–Williams–Watts function) is arbitrary, so that the determination of this distribution is similar to an adjustment of a parameter whose physical significance is ignored.

Here we present a number of experimental results on isothermal ageing for a very wide range of ageing temperature. To provide both a good description of the experimental results obtained by different techniques (d.s.c., dynamic mechanical spectrometry) and a physical interpretation of structural relaxation, an alternative theory is proposed[6–8]. This approach consists of a unique formalism, each parameter of which has a physical meaning. A previous work[9] has shown that physical ageing carried out at a temperature far below T_g induces changes in the dynamic mechanical properties. The aim of this work is to show that this theory applicable above T_g[6,10–12] can take into account the observed phenomena during structural relaxation appearing in a temperature range from below but close to T_g down to far below T_g. Moreover, the effects of structural relaxation on dynamic mechanical and thermodynamic properties are compared.

* Present address: LMM URA 507, INSA 69621, Villeurbanne Cedex, France
† To whom correspondence should be addressed

EXPERIMENTAL

Two different samples of poly(methyl methacrylate) (PMMA) have been studied: one obtained from Röhm and Haas Co. (Germany) and the other provided by Norsolor Co. (France). Their calorimetric glass transition temperatures (value obtained when the metastable equilibrium is reached[11]), measured at a heating rate of 10 K min^{-1} on an as-received sample, are 396 and 404 K respectively. Their molecular weight M_w is 400 000 and 67 000 respectively.

Thermal treatments were performed as follows (see *Figure 1*):

(I) The sample was heated up to 410 K, which is above the glass transition temperature, in an oven and kept at this temperature for more than 15 min. To ensure that the thermodynamic and structural states of the samples when cooled from above T_g to 125 K were identical in all cases, cooling for the thermal treatment of the sample was done at a rate v_q.

(II) Isothermal ageing was performed at a temperature T_a for a certain time t_a.

(III) Then the dynamic or calorimetric measurements were carried out on increasing temperature at a rate v_m.

The values of v_q and v_m corresponding to both mechanical and calorimetric techniques used in this study are given in *Figure 1*.

The structural state used as a reference corresponds to a sample that has not undergone stage (II) of isothermal ageing and will therefore be named as the unaged sample. The other structural states will be referred to as aged samples with definite T_a and t_a.

For dynamic mechanical measurement purposes, the sheets of PMMA were cut into bars of about $2 \times 6 \times 45$ mm^3 dimensions. The real and imaginary parts of the shear modulus (G' and G'' respectively) and the loss tangent $\tan \phi$ (G'/G'') were measured by means of an inverted forced torsional oscillation pendulum[13]. To avoid contamination of the samples by moisture, all measurements and ageing were done in hermetically sealed conditions.

For calorimetric measurement purposes, we used small samples of about 40 mg. Their specific heat C_p was measured by d.s.c., with a Mettler TA 3000 instrument.

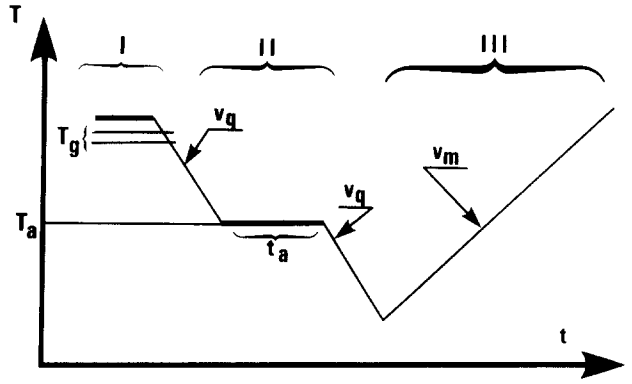

Figure 1 Different stages of thermal treatments undergone by the samples: (I) rapid cooling at a rate v_q after at least 15 min above T_g; (II) static stage, isothermal treatment at T_a for a certain time t_a; (III) dynamic stage, increase of temperature at a rate v_m while carrying out the measurement

	d.s.c.	d.m.s.
Rate of cooling, v_q (K min^{-1})	1000	6
Rate of increase of temperature, v_m (K min^{-1})	10	0.6

RESULTS

The d.s.c. measurements of a PMMA sample with three different thermal histories are shown in *Figure 2a*. Ageing temperatures were 300 K, 322 K and 363 K. The unaged sample does not exhibit a peak in C_p while the aged samples do. These kinds of peaks are rather referred to as pre-peaks as they occur at a temperature noticeably lower than T_g. Ageing at these temperatures, therefore,

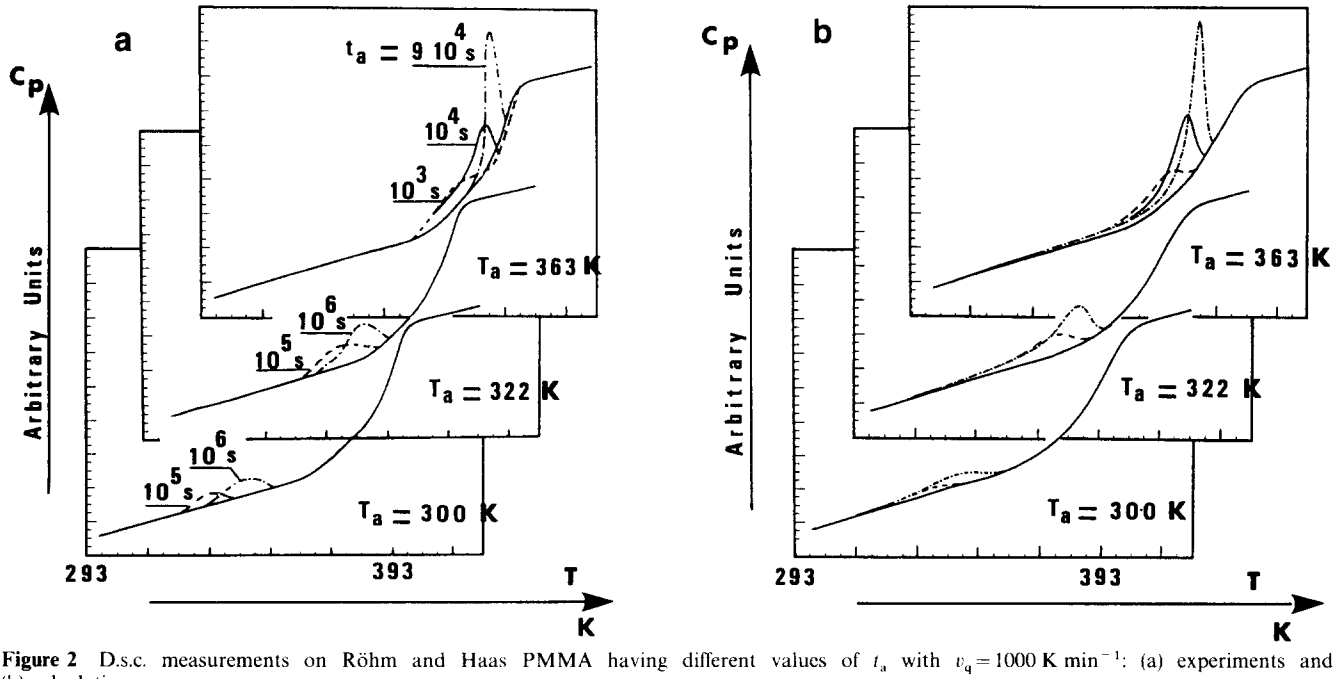

Figure 2 D.s.c. measurements on Röhm and Haas PMMA having different values of t_a with $v_q = 1000$ K min^{-1}: (a) experiments and (b) calculations

produces a pre-peak in C_p that is at a lower temperature the lower the temperature of ageing is. At a given ageing temperature and on increasing ageing time, two simultaneous phenomena are observed: the pre-peak shifts towards higher temperature and its height increases. These general features are in agreement with previous results of Gomez-Ribelles *et al.*[14].

For dynamic mechanical spectrometry (d.m.s.) measurements, ageing has been carried out in the same temperature range as d.s.c. measurements (i.e. 300–363 K). The results are shown in *Figure 3*. Both the α and β relaxations are conveniently seen on a logarithmic scale. The linear scale plot, which is shown as an inset in *Figure 3*, enlarges the features observed near the β relaxation peak and makes them more discernible. This set of plots shows that, on the one hand, at temperatures below 250 K and above about 382 K, the anelastic behaviour at 0.1 Hz of PMMA remains unaffected by its thermal history. On the other hand, there is a wide temperature range below T_g over which structural relaxation occurs. The difference between $\tan\phi$ of unaged and aged samples, or $\Delta(\tan\phi)$, is plotted against temperature in *Figure 4*. The temperatures of the α and β relaxation peaks at 0.1 Hz are indicated by arrows. A peak in $\Delta(\tan\phi)$ appears in all cases of ageing conditions, and this $\Delta(\tan\phi)$ peak shifts to a lower temperature when ageing is done at a lower temperature. The amplitude of these effects ($\Delta(\tan\phi)$)

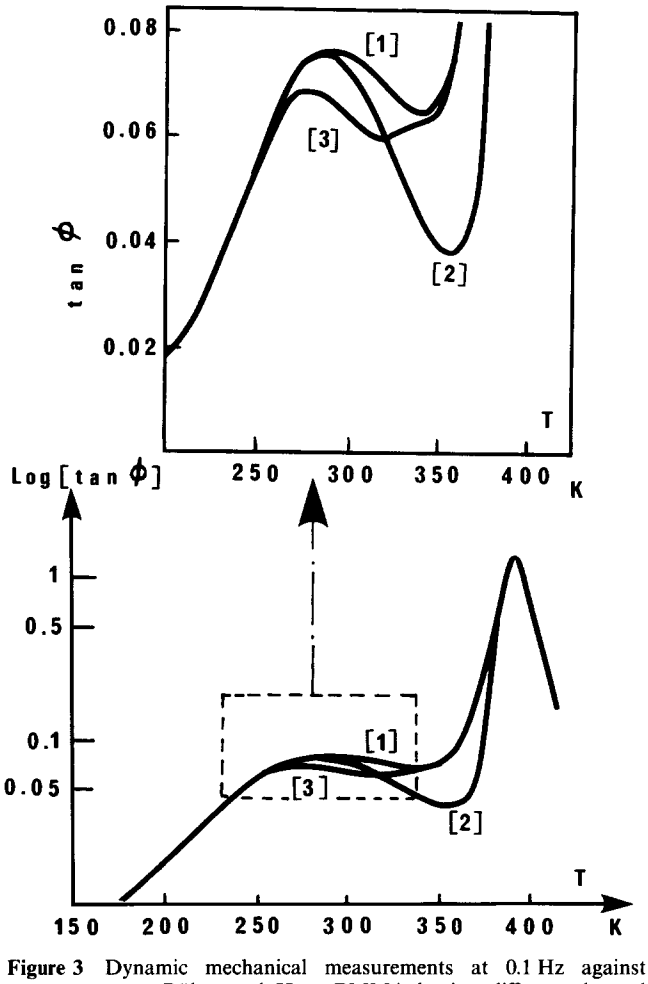

Figure 3 Dynamic mechanical measurements at 0.1 Hz against temperature on Röhm and Haas PMMA having different thermal histories: $v_q = 6$ K min^{-1} and [1] after quenching, [2] $T_a = 363$ K and $t_a = 3.3 \times 10^5$ s, [3] $T_a = 300$ K and $t_a = 2.6 \times 10^6$ s

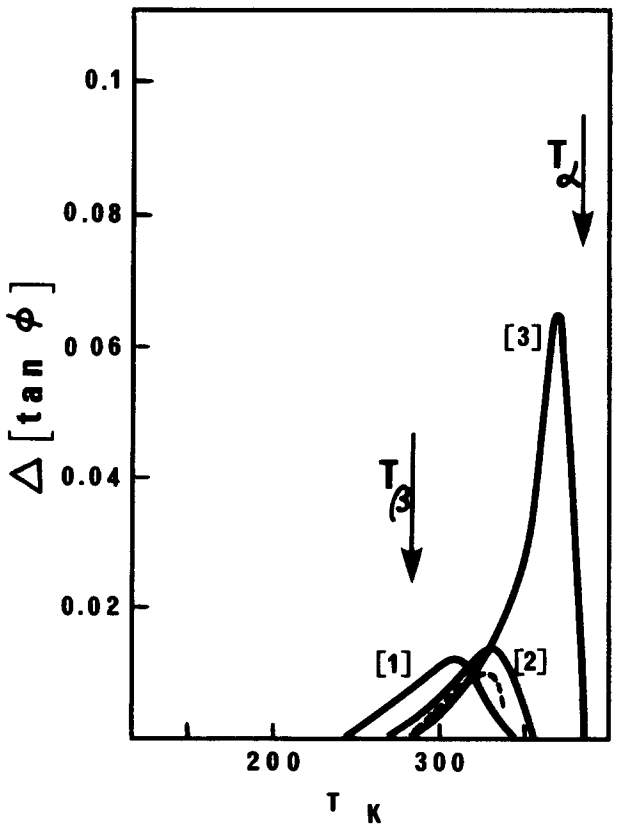

Figure 4 Difference $\Delta(\tan\phi)$ in the mechanical loss tangent of Röhm and Haas PMMA at 0.1 Hz between non-aged and aged samples: [1] 2.6×10^6 s at 300 K, [2] 2.8×10^5 s at 322 K, [3] 3.3×10^5 s at 363 K. The broken curve is discussed in the text

increases with the temperature of ageing. Therefore, the ageing effects observed on both calorimetric and mechanical data follow, at first sight, similar trends[12].

DISCUSSION

We will now focus on dynamic mechanical results, which will first be qualitatively analysed. Then a model of both d.s.c. and d.m.s. results will be presented.

Qualitative analysis of the changes of dynamic mechanical properties during structural relaxation

Although the α relaxation of amorphous polymers is clearly affected by structural relaxation, this is not so for the secondary relaxations, for there are contradictory statements[15–17]. Our results of low-temperature ageing on PMMA provide us with an answer to the following question.

Is β relaxation affected by structural relaxation? The β relaxation of PMMA exhibits a maximum in $\tan\phi$ at about 285 K for a frequency of 0.1 Hz and has a broad distribution of relaxation times[18]. Results of *Figure 3* show that the loss tangent at 0.1 Hz of PMMA remains unaffected by its thermal history below 250 K no matter which temperature of ageing has been chosen. This means that the fastest movements involved in the β relaxation are not sensitive to physical ageing. Therefore, only the structural units having long relaxation times would relax on ageing, which seems very unlikely. This leads us to the idea that the β relaxation is not affected by structural relaxation.

Another way of looking into the question is to examine the plots of $\Delta(\tan\phi)$ on *Figure 4*. According to Johari's criteria[15], if any secondary relaxation is affected by physical ageing, the maxima of $\Delta(\tan\phi)$ and of this relaxation would occur at the same temperature. Since the plots of *Figure 4* exhibit a peak whose maximum does not correspond to the maximum of the β relaxation, it is very unlikely that structural relaxation is originated by a change of the β-relaxation features.

The other possibility is now straightforward: only the α relaxation is affected by structural relaxation. To account for the apparent decrease of the β-relaxation height and temperature due to a modification of the α relaxation, the α relaxation is considered to be stretched towards low temperatures. Let us envisage the convolution of these two relaxation peaks, with only the α peak affected by thermal treatments.

We subtract the β-relaxation contribution calculated according to a previous work[18] from the $\tan\phi$ spectrum for the non-aged sample. This leads to an α-relaxation which is spread towards the β-relaxation temperature range (curve [a] of *Figure 5*). In order to take into account the ageing effects, we now subtract the $\Delta(\tan\phi)$ of *Figure 4* from curve [a]. We obtain curves [b] and [c]. This enables us to underline the idea that structural relaxation affects only the low-temperature tail of the α relaxation. The lower the ageing temperature, the lower is the affected α domain. When both α and β contributions are considered, as shown in the insert of *Figure 5*, the β maximum appears at a higher temperature and its height seems bigger than for the β peak alone. However, the β relaxation has been considered not to be affected by ageing in this curve treatment.

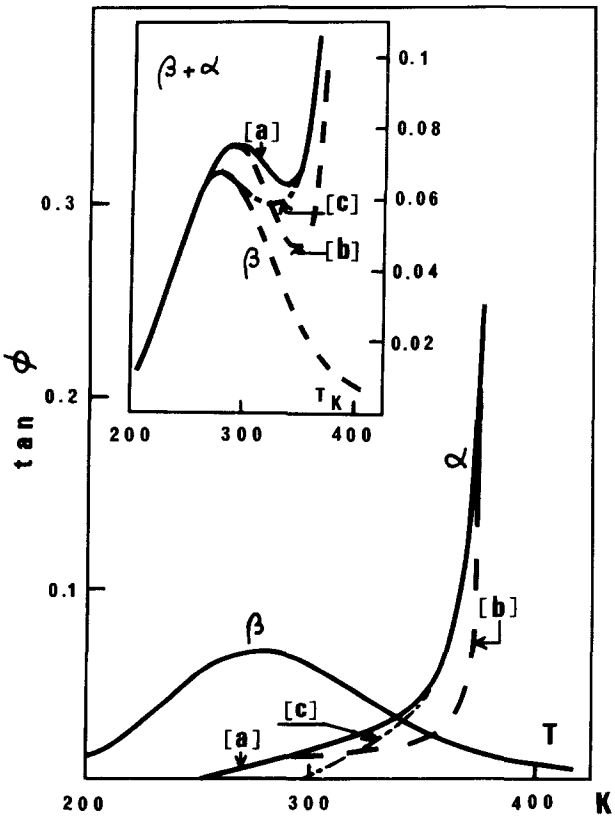

Figure 5 Schematic α and β relaxation peaks at 0.1 Hz. The insert represents the summation of the two thermograms. The β relaxation peak is calculated as in ref. 17 and the α relaxation peak is represented in three cases corresponding to: [a] a rapidly cooled sample $v_q = 6$ K min^{-1}; [b] a sample aged 3.3×10^5 s at 363 K; [c] a sample aged 2.6×10^6 s at 300 K. Use has been made of the results of *Figure 4*

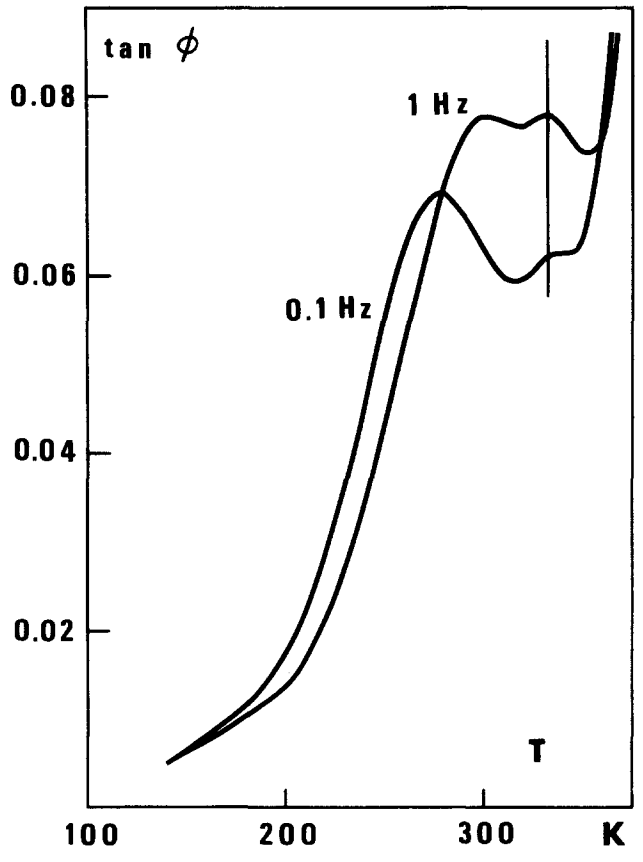

Figure 6 Dynamic mechanical measurements at 0.1 and 1 Hz against temperature on Röhm and Haas PMMA aged 2.6×10^6 s at 300 K

Development of a further maximum between T_β and T_α for low-temperature ageing. Structural relaxation of PMMA during isothermal ageing at 300 K (about 100 K below T_g) produces a manifestation in its anelastic behaviour that has not been observed before (*Figure 6*): the recovery at about 340 K of the $\tan\phi$ curve of a non-aged sample between the β and α relaxation peaks. This recovery occurs such as to produce a maximum at about 330 K, a temperature that our measurements at 0.1 and 1 Hz have shown to be independent of the frequency (*Figure 6*).

To examine whether or not the new maximum that shows up at temperatures between the β and α relaxation peaks is affected by thermal cycling below T_g, a separate experiment was carried out on a sample of the Norsolor PMMA (*Figure 7*). The thermal treatments were the same as before (*Figure 1*) with $T_a = 300$ K and $t_a = 4.4 \times 10^6$ s, but the measurement was carried out up to the domain where the maximum showed up, i.e. 336 K, then stopped (curve [b], first measurement). The sample was thereafter immediately cooled to 125 K and $\tan\phi$ was measured again on increasing temperature at the same rate of $v_m = 0.6$ K min^{-1} (curve [c], second measurement). These results are compared with the one obtained on a non-aged sample (curve [a]) in *Figure 7*. These data clearly show that heating the PMMA sample, after ageing at 300 K, to a temperature far below T_g (336 K) causes this extra

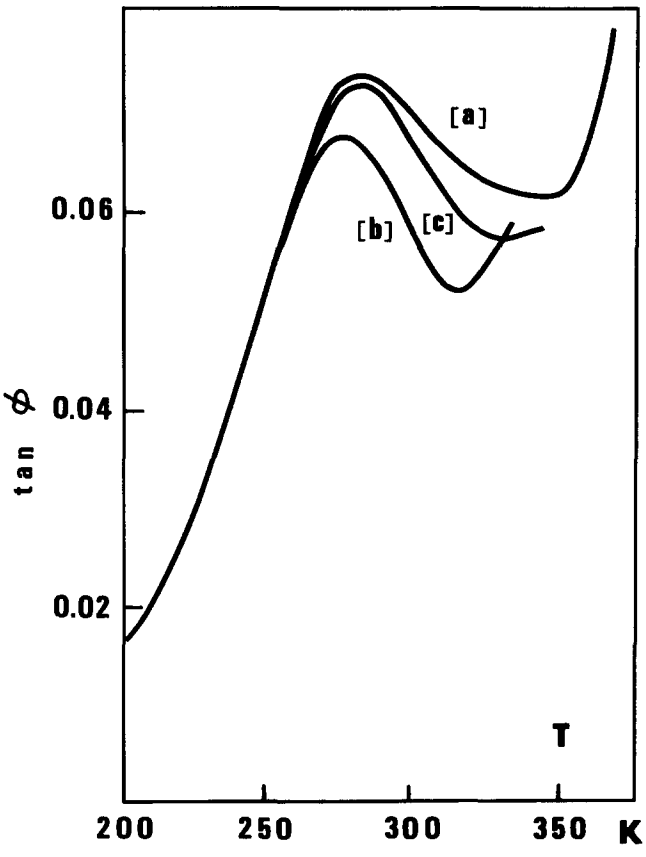

Figure 7 The tan ϕ at 0.1 Hz of Norsolor PMMA measured for: [a] a rapidly cooled state, [b] a sample aged 4.4×10^6 s at 300 K. When the sample had reached 336 K, the experiment was stopped, the sample was immediately cooled down to 125 K and measured again [c] up to 346 K

maximum to vanish. It also raises the height of tan ϕ in the β relaxation region and apparently shifts the β maximum to a higher temperature. This means that the extra maximum is caused by the effect of the heating during the d.m.s. measurements after ageing at 300 K. This heating partly erases the previous ageing effect as the shape of curve [c] approaches that of an unaged sample (curve [a]). The extra maximum is not an intrinsic property of the polymer, i.e. not a true relaxation peak.

Such a specific experiment underlines the gradual and spontaneous changes of the structural state during the measurements. The difference between curves [a] and [c] in *Figure 7* is plotted as a broken curve on the $\Delta(\tan\phi)$ plot of *Figure 4*. This curve is located close to curve [2] of *Figure 4*; it leads us to believe that the heating during the measurement of curve [b] corresponds to a thermal treatment whose effects are comparable to that of an isothermal ageing at a temperature of about 325 K.

Physical modelling of structural relaxation: formalism

The physical interpretation of structural relaxation is the subject of many studies[19,20], amongst which is the one currently developed in our laboratory[6–8]. The latter is based on the quasi-point-defect theory[6,7]. Let us remark that the quasi-point-defect concept is now often considered in kinetic models of liquid–glass transition[21,22].

We consider the polymeric system as a disordered arrangement of structural units, each unit being trapped in a cage formed by its neighbouring units. In such a description, local sites where the density is higher (d^+) or lower (d^-) than the average density are referred to as quasi-point defects. The concentration of defects, when the system is at equilibrium, is given at each temperature by:

$$C_d = \frac{1}{1+\exp(\Delta S_F/k)\exp(\Delta H_F/kT)} \quad (1)$$

where ΔS_F and ΔH_F are respectively the average entropy and enthalpy of formation of a defect.

When the sample is rapidly cooled from above T_g, the concentration of defects is somewhat frozen-in. During physical ageing, the system tends towards its new concentration of equilibrium. We therefore consider the following equation:

$$2\,NS \underset{2}{\overset{1}{\rightleftharpoons}} d^+ + d^- + \Delta G \quad (2)$$

with NS representing a normal site.

Structural relaxation consists in eliminating the defects and deals therefore with an evolution in direction 1 of equation (2). Owing to potential anharmonicity, this evolution leads indeed to a higher density[11], as observed experimentally. The defect concentration decreases during time of ageing according to the differential equation:

$$\frac{dC_d(t,T)}{dt} = -\frac{C_d(t,T)-C_d(\infty,T)}{\tau_{rs}(t,T)} \quad (3)$$

where $C_d(t,T)$ is the concentration at time t and temperature T, $C_d(\infty,T)$ is the equilibrium concentration at T (equation (1)) and $\tau_{rs}(t,T)$ is the time characteristic of the structural relaxation and can be taken similar to the time for molecular mobility τ_{mol} (ref. 11).

The mechanism of annihilation of defects has been described in terms of a diffusion process[10] resulting from hierarchically correlated movements[23]: a given molecular movement[21,24] is possible only if previous elementary movements have occurred. This leads to the expression for τ_{mol}, namely:

$$\tau_{mol} = t_0(\tau_\beta/t_0)^{1/b} \quad (4)$$

where b is the correlation factor, τ_β is the relaxation time for the β relaxation, with $\tau_\beta = \tau_0\exp(-U_\beta/kT)$, where τ_0^{-1} is the frequency factor and U_β the activation energy of the β relaxation, and t_0 is a scaling time factor.

The correlation factor b relates therefore to the hierarchical correlation of the molecular motion; b is between 0 and 1. If $b=0$, the correlation is maximum, τ_{mol} becomes infinity (equation (4)) and no motion is possible. If $b=1$, there is no correlation and the movement of a structural unit occurs independently of the others. Then, b is a structural parameter: the higher the disorder, the larger is the value of b. Thus b is directly related to the defect concentration C_d. The following expression:

$$b = 1/[1+B\exp(-AC_d)]$$

was proposed[8,11] to connect b to C_d in the vicinity of T_g. As the defects are randomly distributed in the amorphous polymer, their concentration is not rigorously homogeneous in the whole sample. The correlation effects are therefore different from one place to another: this is described by a distribution of the correlation factor b. To take into account this physical reality, we consider a

simple Gaussian distribution of $1/b$ (ref. 11). Such a formalism provides also a Gaussian distribution of the logarithmic molecular relaxation time $\ln \tau_{mol}$, thanks to equation (4). A small value of $1/b$ (or $\ln \tau_{mol}$) corresponds to a high molecular mobility, and a high value of $1/b$ (or $\ln \tau_{mol}$) corresponds to a low molecular mobility. For simplification, we consider the case of a Gaussian distribution of $1/b$ with a temperature-independent width B_{Gauss}. Actually, for numerical calculation purposes, we consider a finite number of values for $1/b$. To do so, let us envisage N families of defects referred to by a j index. Equations (3) and (4) become now:

$$\frac{dC_{dj}(t,T)}{dt} = -\frac{C_{dj}(t,T) - C_{dj}(\infty,T)}{\tau_{mol,j}(t,T)} \quad (5)$$

with

$$C_d = \Sigma_j C_{dj}$$

and

$$\tau_{mol,j}(t,T) = t_0(\tau_\beta/t_0)^{1/b_j} \quad (6)$$

Equations (5) and (6) refer to the evolution of the microstructure of a system with time, owing to a set of N equations. We can consequently describe the evolution of systems during either isothermal ageing or under non-isothermal treatment, for example during rapid cooling or increase of temperature at a determinate rate. In the latter cases, we simply consider these changes of temperature as a succession of isothermal stages. The time of each isothermal stage and the variation of temperature between two stages was chosen to obtain a good enough precision of the calculations.

At this stage, it is noteworthy that the concentration of defects C_d is proportional to the enthalpy through:

$$H_j(t,T) = N_a \Delta H_F C_{dj}(t,T)$$
$$H(t,T) = \Sigma H_j(t,T) \quad (7a)$$

Then, C_p is calculated from the enthalpy through:

$$C_{pj}(T) = \frac{dH_j(t,T)}{dT}$$
$$C_p(T) = \Sigma C_{pj}(T) \quad (7b)$$

We have considered here 21 families of defects. Also, to simplify the representation, we have named each family by its number from 0 to 20. The plots of the defect concentration C_{dj} against j are referred to as histograms and their evolution throughout the thermal treatments will be analysed now. Although the abscissa of the histograms remains the same, this does not mean that $1/b_j$ remains constant all along the calculations. In fact, the average value of $1/b$ is time- and temperature-dependent, since it is related to C_d.

The numerical values of the different parameters are listed in *Table 1*. These values are either calculated directly from experimental data (ΔS_F, ΔH_F, τ_0, U_β, b_0, A) or are adjustable parameters (τ_0, B_{Gauss}). Determination of the value of these parameters is given in ref. 25. These parameters are kept constant whatever thermal treatment or experimental technique is considered.

Physical modelling of structural relaxation: discussion

According to this formalism, let us now envisage the evolution of the concentration of defects C_{dj} with thermal history. We will consider the three stages shown in *Figure 1* to perform the calculations, i.e. cooling, isothermal ageing and heating for measurements.

Effect of cooling. At any temperature, the system possesses a concentration of equilibrium C_d defined through equations (1) and (5) and described by a Gaussian distribution. This distribution is shown on *Figure 8* for temperatures of 410 K and 363 K. The area under these histograms corresponds to the total defect concentration at each temperature; it is unsurprisingly greater at 410 K than at 363 K.

If we compare the equilibrium histograms with the one obtained after simulation of a rapid cooling from 410 K to 363 K at the rate $v_q = 1000$ K min^{-1}, it is to be seen (*Figure 8*) that the concentration of each family of defects has evolved and tends towards its equilibrium at 363 K.

Table 1 Numerical values for the parameters used in the calculations

ΔS_F (kJ mol^{-1} K^{-1})	ΔH_F (kJ mol^{-1})	τ_0 (s)	U_β (kJ mol^{-1})
3.23	13.4	2.6×10^{-16}	77.8
t_0 (s)	B	A	B_{Gauss}
4.5×10^{-9}	52	11.35	0.6

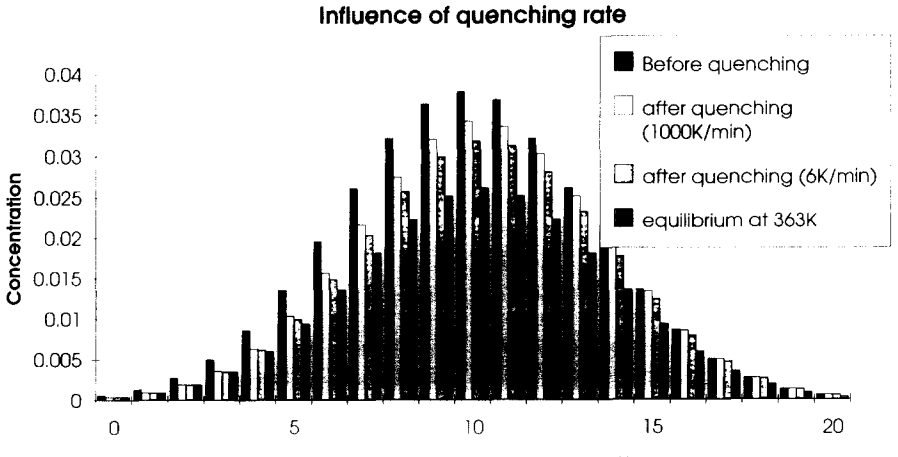

Figure 8 Effect of rapid cooling on the population of defects for different cooling rates

However, the kinetics of this evolution depends upon the intrinsic mobility of each family: families 0 to 4 have reached their equilibrium at 363 K while the other families have not. Besides, the relative difference with the concentration at equilibrium is greater when the family is less mobile. Briefly stated, the more mobile a defect is, the closer it tends towards its equilibrium.

Comparison of results with v_q of 1000 and 6 K min^{-1} clearly shows that the cooling rate is a crucial factor to determine the population of each family after cooling. Indeed, a slow cooling allows an easier evolution towards equilibrium.

The effects of cooling on the population of defects are summarized as follows:

(i) Cooling the system from above T_g to a certain temperature T_a allows it to evolve towards the equilibrium configuration at T_a, but only to the extent allowed by the mobility of each family.

(ii) This evolution has a kinetic aspect so that a very rapid cooling or quenching enables the system to be frozen in a configuration close to the equilibrium configuration above T_g. On the other hand, an extremely slow cooling would allow the system to remain at equilibrium all through the cooling. These two cases are the extreme situations and are, of course, never experimentally possible.

(iii) The defects behave quite differently depending on their mobility.

Effect of isothermal ageing—static effect. We will now consider the evolution of the defect concentration during isothermal ageing of 10^6 s at a certain temperature T_a and after cooling at a rate of 1000 K min^{-1}. *Figure 9* shows the histograms obtained for three temperatures of ageing: 363, 322 and 300 K.

First, let us examine the histograms after cooling: they are identical at 322 and 300 K. This means that, during cooling at 1000 K min^{-1}, the system does not evolve any more between 322 and 300 K.

We compare now the evolution towards equilibrium for different ageing temperatures. The defects that have reached their equilibrium concentration are:

at 363 K, the numbers 0 to 9 (*Figure 9a*)

at 322 K, the numbers 0 to 5 (*Figure 9b*)

at 300 K, the numbers 0 to 3 (*Figure 9c*)

Therefore, structural relaxation affects a greater number of defect families when the temperature of ageing is higher. Nevertheless, the treatment of 10^6 s at 363 K does not enable the system to reach a complete equilibrium. At the lower temperature of ageing considered here (300 K), only the more mobile defects are noticeably affected by ageing.

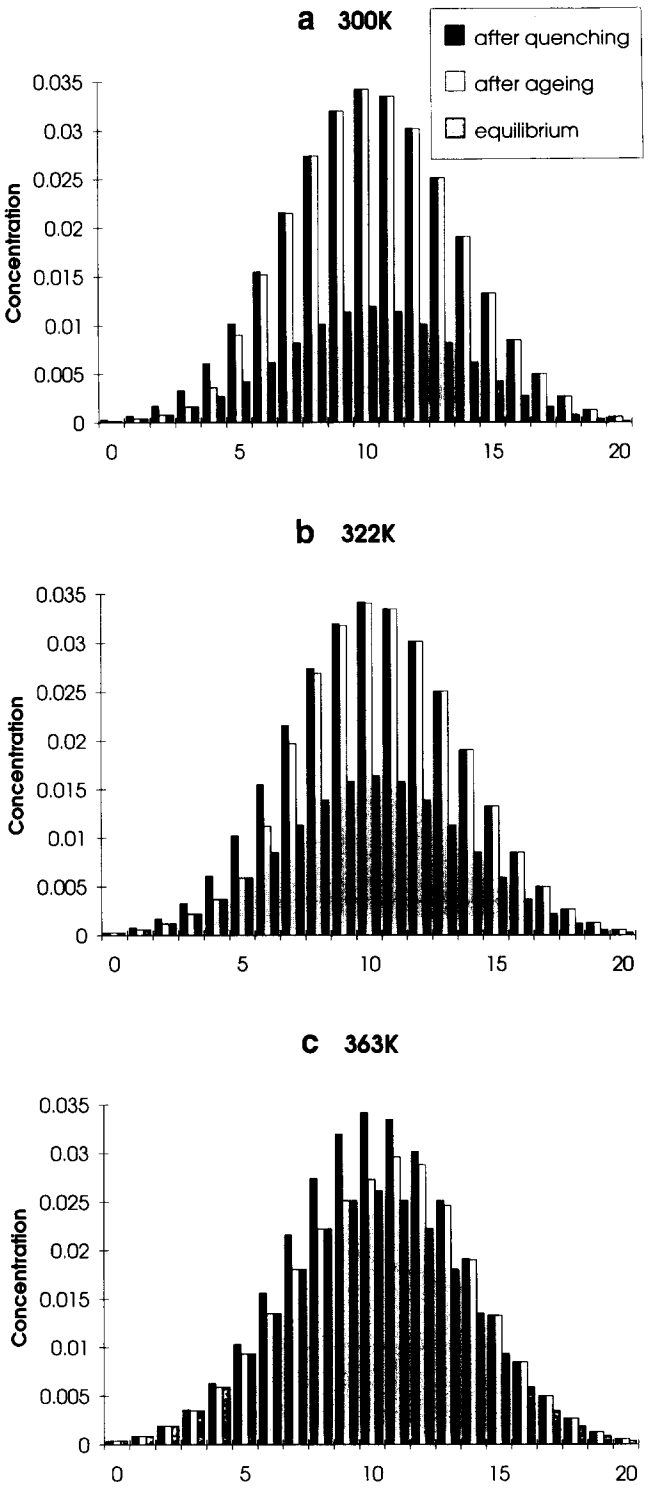

Figure 9 Evolution of the population of defects during isothermal ageing during 10^6 s for different ageing temperatures: (a) 363, (b) 322 and (c) 300 K

Effect of increase in temperature—dynamic effect. Though it is generally possible to measure the evolution of a property with time during isothermal ageing, some experimental techniques require us to study the phenomena by performing an increase of temperature. This is typically the case for d.s.c. Furthermore, this increase of temperature itself constitutes part of the thermal history of the sample, which is likely to evolve during the measurement.

We have considered the evolution of the defect concentration with temperature during the measurement. The treatment simulated before the measurement consists of cooling at a rate of 1000 K min^{-1} and an isothermal plateau at 363 K for 9×10^4 s. We now focus on two particular types of defect: families 7 and 13 that have the same concentration at equilibrium (broken line on *Figure 10a*) but whose evolutions are very much different. The plot of the concentration of defects against temperature, as we pointed out with equation (7), is proportional to the one of the enthalpy (*Figure 10a*).

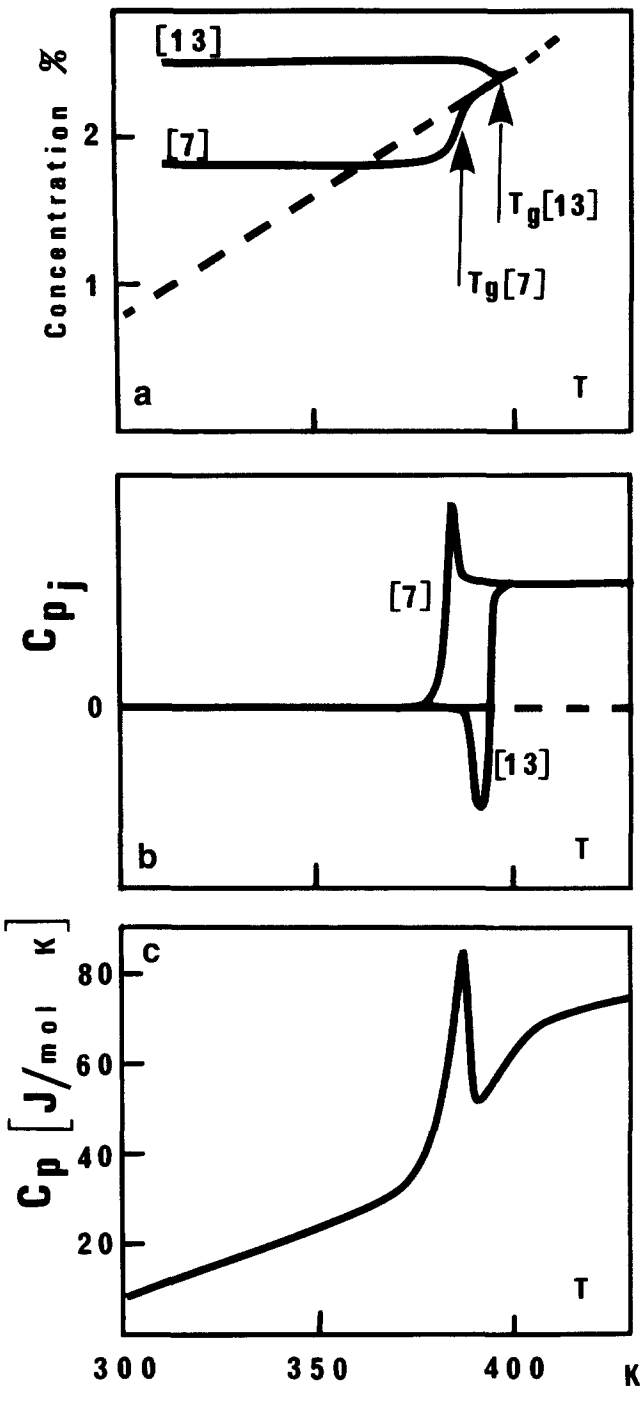

Figure 10 Dynamic effects on the population of defects: (a) evolution of the population of families number 7 and 13; (b) summation of both evolutions ($C_{d7}+C_{d13}$); (c) resulting C_p curve when all the families as well as the phonon effect are considered

Let us first observe the evolution with temperature of population number 7. The concentration remains constant until 380 K and then quickly (in 8 K) reaches its equilibrium concentration and follows it at higher temperatures. We explain such a behaviour as follows:

(i) At low temperature, these defects are in excess of the equilibrium concentration (broken line represents the equilibrium concentration). Nevertheless, their concentration cannot diminish because their mobility is not high enough.

(ii) From 363 to 380 K, the concentration of the defects is lower than the equilibrium one but still the mobility does not enable the family to evolve towards equilibrium.

(iii) From 380 to 388 K, as the mobility is sufficient, the concentration rapidly increases and then reaches equilibrium. This phenomenon corresponds to a structural recovery. The maximum rate of this evolution is estimated for a temperature of about 386 K, which constitutes the maximum of the specific heat plot (*Figure 10b*).

(iv) The glass transition temperature corresponding to the seventh family is referred to here as $T_g(7)$. This temperature corresponds to the achievement of the metastable equilibrium of this family. Under these conditions, $T_g(7)$ is equal to 388 K. At higher temperature, the defects of type 7 follow the equilibrium concentration.

If we now envisage the case of population number 13, the behaviour is quite different. The concentration remains constant until 390 K, then decreases until 396 K, the temperature at which the equilibrium is reached. We analyse this behaviour as follows:

(i)These defects are less mobile than the defects number 7, so that the concentration where they are frozen in, after ageing, is higher. The evolution is then possible only at very high temperature. The variation of concentration is seen at a temperature higher than 390 K whereas it appears at 380 K for the family number 7.

(ii) The remarkable effect from 390 K is a diminution of the concentration of defects up to 396 K. This mechanism corresponds to a physical ageing phenomenon, which occurs during the increase of temperature between 390 and 396 K. This effect, purely dynamic, is possible for less mobile units because they have a higher concentration than equilibrium when their motion becomes possible.

(iii) The glass transition temperature $T_g(13)$ under these conditions corresponds to 396 K. The defects of type 13 have from then on a concentration corresponding to the equilibrium.

It is now straightforward to interpret the curves $C_p(t,T)$ corresponding to the same thermal treatment. Indeed, C_p corresponds to the derivative of C_d with temperature according to equation (7). The specific heat of each family is proportional to the slope of the concentration at each temperature, so that the curves of $C_{pj}(T)$ are obtained for each family on *Figure 10b*.

(i) Nothing evolves at low temperature, so that C_{pj} is equal to zero.

(ii) Population number 7 begins to tend towards its equilibrium at 380 K, as is seen by an evolution of $C_p(7)$. $C_p(7)$ increases until a maximum corresponding to the inflection point of the concentration curve and then decreases down to a constant value corresponding to the slope of the quasi-straight line of equilibrium concentration.

(iii) Population number 13 begins to evolve at about 388 K by diminishing and then reaches its equilibrium: curve $C_p(13)$ becomes negative during physical ageing and then reaches the constant value corresponding to the slope of the quasi-straight line of equilibrium concentration.

For generalization, we now consider the whole set of families of defects. The more mobile families reach their equilibrium in an identical way to family 7, whereas the

less mobile families behave similarly to family 13. The temperature at which the evolution is triggered is lower when the mobility is greater. Therefore it is obvious that the first types of defects reaching their equilibrium correspond to family 0. In contrast, the last types of defects reaching their equilibrium correspond to family 20.

Features of the pre-peak of $C_p(T)$ simulated in *Figure 10c* have been obtained by considering the entire set of families of defects and by adding the phonon effect (it has been estimated by a linear variation of C_p with temperature). Two competitive effects are to be seen as summarized on *Figures 10a* and *10b*.

(i) The steep increase of C_p from about 380 K reflects the effect of evolution towards equilibrium of the more mobile units through a recovery phenomenon. This recovery has the greatest rate when C_p exhibits its maximum.

(ii) The diminution of C_p between about 388 and 392 K reflects the slowing down of this kinetics. Moreover, because of the ageing of the less mobile defects during the increase in temperature, a minimum appears in the C_p curve.

When ageing is performed at lower temperatures compared to T_g, same phenomena are to be seen on the curve $C_p(T)$ (*Figure 2*) with the noticeable differences:

(i) The C_p pre-peak appears at a lower temperature. Indeed, at such a low-temperature ageing, the global mobility of the system is kept very high because evolution towards equilibrium occurs to a very small extent. Therefore, during the d.s.c. heating, the system reaches its equilibrium more easily (i.e. at a lower temperature).

(ii) The amplitude is smaller. The height of the pre-peak is a function of the rate at which the families of defects reach their equilibrium concentration. In that case, this difference is small because the evolution involves only the most mobile units.

We do not consider here the effect of duration of ageing on the C_p peak in detail. However, from the above explanation, it is quite straightforward that the C_p pre-peak is higher when the ageing lasts longer.

When ageing is performed close to but below T_g, all the families of defects significantly evolve towards equilibrium during isothermal ageing. Their concentrations during heating are all lower than the equilibrium one and the trigger for reaching the equilibrium concentration occurs later, i.e. at a higher temperature. Experimental results then exhibit peaks of C_p instead of pre-peaks[14].

All the mechanisms described above lead to the experimental observations and enable a physical interpretation of the results. Let us now compare our calculations with the experimental results obtained by either calorimetric or dynamic mechanical techniques.

Specific-heat measurements are simulated owing to the determination of C_{dj} as previously described and equation (7). *Figure 2* compares experimental results with the calculations. In every case of thermal treatment, the position in temperature, height and width of the pre-peak are comparable. In the same way, we have compared experimental results of other authors who have performed isothermal ageing at noticeably higher temperatures[14] (to obtain C_p peaks instead of pre-peaks in our case). The simulation also describes this kind of result well. It appears therefore that this model is capable of describing the calorimetric results of structural relaxation in a very large range of temperature and time of ageing and that it also provides a physical interpretation of the results in terms of an evolution of defect concentration. It is noteworthy that this model is not thermo-rheologically simple, as the exponent $1/b$ is not constant but depends on the thermal history through the defect concentration.

For simulation of the dynamic mechanical results, we consider the modification of the α relaxation on ageing. The compliance of the α relaxation has three components, respectively an elastic, an anelastic and a viscoplastic one[6,10]:

$$J_\alpha^*(i\omega)=\frac{1}{G_e}\left[1+(i\omega\tau_{mol})^{-b}+C(i\omega\tau_{mol})^{-b'}\right] \quad (8)$$

where ω is the angular frequency, G_e is the elastic modulus, τ_α is proportional to τ_{mol}, C is a constant[10] and b' is related to the amount of entanglements[10].

However, this formula does not take into account the distribution in $1/b$ (ref. 26) although we have shown that this distribution is a critical factor to explain the d.s.c. measurements. Then alternatively, the following expression, similar to the one proposed by Perez[11], is used:

$$J_\alpha^*(i\omega)=\frac{1}{G_e}\left(1+C\sum_j\frac{1-i\omega\tau_{mol,j}}{1+(\omega\tau_{mol,j})^2}+(i\omega\tau_m)^{-b'}\right) \quad (9)$$

where τ_m is the average of $\tau_{mol,j}$. In this expression, the distribution of the relaxation times (or of $1/b$) is taken into account by the summation on j.

In addition, we also consider that all the movements involved in the α relaxation, i.e. from the elementary one, τ_β, up to τ_{molj}, contribute to the anelastic component. This is taken into account by a distribution of τ_α between τ_β and $\tau_{mol,j}$ according to a semi-Gaussian curve, the maximum of which is taken at τ_{molj}.

Figure 11 gives the calculations carried out during d.m.s. simulations for samples initially quenched (curve [1]) and after ageing at 363 K (curve [2]) and 300 K (curve [3]). We have taken into account the β relaxation by adding the compliance $J_\beta^*(i\omega)$ as previously determined

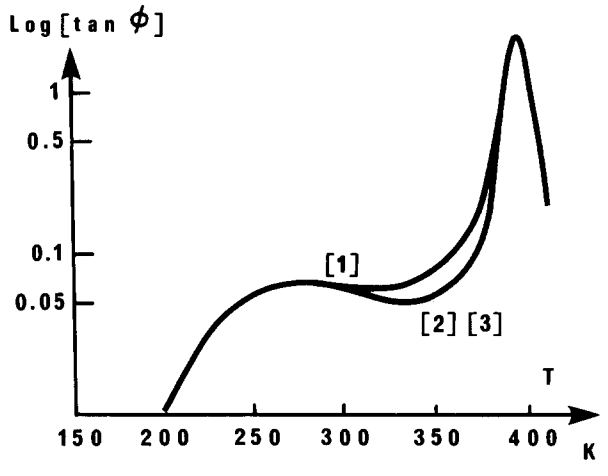

Figure 11 Dynamic mechanical calculations with $v_q = 6$ K min^{-1} and: [1] after quenching; [2] $T_a = 363$ K and $t_a = 3.3 \times 10^5$ s; [3] $_a = 300$ K and $t_a = 2.6 \times 10^6$ s

in another work[18]. Calculated curves of *Figure 11* are to be compared with experimental curves of *Figure 3*.

The ageing effects at 363 K are well described by the simulation. In particular, the temperature range where physical ageing influences the mechanical properties is identical. Both experimental and calculated results exhibit a temperature of about 382 K where the unaged and aged at 363 K $\tan\phi$ curves meet. This constitutes the glass transition temperature of the system, i.e. the temperature at which, under these conditions (v_q = 6 K min^{-1} and v_m = 0.6 K min^{-1}), the whole system has reached its equilibrium. Moreover, the amplitude of the decrease of $\tan\phi$ is comparable to the experimental one. Structural relaxation phenomena observed for ageing temperatures close to T_g are interpreted in a self-consistent way by considering physical mechanisms as annihilation of defects.

However, ageing effects at 300 K are not satisfactorily described by the model. Indeed, our simulations do not reproduce the features we observed through d.m.s. characterization of 300 K ageing. As a matter of fact, simulations do not exhibit any evolution of the defect concentration during ageing at 300 K, so that the model predicts that no pre-peak in d.s.c. would be seen for an experiment with $v_q = 6$ K min^{-1} and $T_a = 300$ K. Such a specific d.s.c. experiment has been performed and no detectable modification of the C_p curve was seen after ageing, confirming that the concentration of defect remains unchanged during an isothermal ageing at 300 K.

It is now quite clear that, under the same ageing conditions, d.m.s. measurements can be affected when d.s.c. measurements are not. Low-temperature ageing therefore appears to show a decrease of molecular mobility when the defect concentration remains unchanged.

Let us now envisage some possible explanation of this apparent inconsistency. We do think of the occurrence, especially during ageing at low temperature, of some kind of local molecular rearrangements in domains where the most mobile defects are located. These local rearrangements would not allow a real elimination of defects but would nevertheless decrease the molecular mobility.

This decrease in molecular mobility implies an increase of $\tau_{mol,j}$, which can be envisaged in two ways (see equation (6)):

(i) An increase of τ_β through U_β, the potential barrier associated with the defect. In fact, a very small change in U_β can induce a noticeable variation of $\tau_{mol,j}$. For example, a variation of U_β of 0.3% leads to a variation of $\tau_{mol,j}$ of about 15 to 20% (for the most mobile defects). However, this first hypothesis seems very unlikely since the low-temperature part of the β relaxation peak is experimentally unaffected, even for ageing carried out at low temperature.

(ii) A decrease of b_j, the correlation factor. For example, a variation of b_j as small as 1% leads to a variation of $\tau_{mol,j}$ of about 20%. This hypothesis seems conceivable and will be investigated further in future work.

CONCLUSION

We have obtained experimental results on physical ageing by means of two different techniques. This procedure reveals noticeable differences in the behaviour of an amorphous polymer whether the temperature of ageing is close to or far below T_g.

For ageings carried out at temperatures below but not too far from T_g ($T_g - 30$), experimental results obtained from both techniques are consistent with each other. The β relaxation remains unaffected by physical ageing.

All the data are well described by a physical model based on the existence of quasi-point defects. One of the main features of this model is to use a single set of parameters whatever the thermal history and the experimental technique considered, each parameter having a physical meaning. The observed phenomena (d.s.c. pre-peak, decrease of the low-temperature tail of the α relaxation, etc.) can be understood owing to the evolution of the distribution of the quasi-point defects towards their equilibrium concentration.

For ageings carried out at temperatures far below T_g ($T_g - 100$) and after slow cooling, no evolution of the d.s.c. curve is seen. This is in agreement with the simulation that predicts no change of defect concentration during such ageing. However, the molecular mobility is noticeably decreased: the very low-temperature part of the α relaxation is lowered. A recovery of this mobility occurs during the d.m.s. experiment, leading to the observation of a maximum. We interpret this loss of mobility in terms of local molecular rearrangements.

REFERENCES

1 Kovacs, A. J., Aklonis, J. J., Hutchinson, J. M. and Ramos, A. R. *J. Polym. Sci., Polym. Phys. Edn.* 1979, **17**, 1097
2 Tool, A. Q. *J. Am. Ceram. Soc.* 1946, **29**, 240
3 Narayanaswamy, O. S. *J. Am. Ceram. Soc.* 1971, **54**, 491
4 Hodge, I. M. *Macromolecules* 1987, **20**, 2897
5 Adam, G. and Gibbs, J. H. *J. Chem. Phys.* 1965, **43**, 139
6 Perez, J., Cavaillé, J. Y., Etienne, S. and Jourdan, C. *Rev. Phys. Appl.* 1988, **23**, 125
7 Diaz-Calleja, R., Perez, J., Gomez-Ribelles, J. L. and Ribes-Greus, A. *Makromol. Chem., Macromol. Symp.* 1989, **27**, 289
8 Vigier, G. and Tatibouët, J. *Polymer* 1993, **34**, 4257
9 Muzeau, E., Cavaillé, J. Y., Vassoille, R., Perez, J. and Johari, G. P. *Macromolecules* 1992, **25**, 5108
10 Cavaillé, J. Y., Perez, J. and Johari, G.P. *Phys. Rev. (B)* 1989, **39**, 2411
11 Perez, J. 'Physique et Mécanique des Polymères Amorphes', Lavoisier, Paris, 1992
12 Perez, J., Etienne, S. and Tatibouët, J. *J. Phys. Stat. Sol. (a)* 1990, **121**, 129
13 Etienne, S., Cavaillé, J. Y., Perez, J., Point, R. and Salvia, M. *Rev. Sci. Instrum.* 1982, **53**, 1261
14 Gomez-Ribelles, J. L., Ribes-Greus, A. and Diaz-Calleja, R. *Polymer* 1990, **31**, 223
15 Johari, G. P. *J. Chem. Phys.* 1982, **77**, 4619
16 Struik, L. C. E. *Polymer* 1987, **28**, 57
17 Dean, G. D., Read, B. E. and Small, G. D. *Plast. Rubb. Process. Applic.* 1988, **9**, 173
18 Muzeau, E., Perez, J. and Johari, G. P. *Macromolecules* 1991, **24**, 4713
19 Moynihan, C. T., Macedo, P. B., Montrose, C. J., Gupta, P. K., DeBolt, M. A., Dill, J. F., Drake, P. W., Easteal, A. J., Elterman, P. B., Moeller, R. P., Sasabe, H. and Wilder, J. A. *Ann. NY Acad. Sci.* 1976, **279**, 15
20 Hodge, I. M. and Berens, A. R. *Macromolecules* 1982, **15**, 762
21 Fredericson, G. H. and Brower, S. A. *J. Chem. Phys.* 1972, **84**, 3351
22 Soules, T. F. and Markovsky, A. *J. Chem. Phys.* 1987, **86**, 5874
23 Perez, J. *Polymer* 1988, **29**, 483
24 Palmer, R. G., Stein, D. L., Abrahams, E. and Anderson, P. W. *Phys. Rev. Lett.* 1984, **53**, 958
25 Muzeau, E., PhD Thesis, Institut National des Sciences Appliquées de Lyon et Université Lyon I, 1992
26 Perez, J. and Cavaillé, J. Y. *Trends Polym. Sci.* 1991, **2**, 63